ELSEVIER

Contents lists available at ScienceDirect

Ceramics International

journal homepage: www.elsevier.com/locate/ceramint





Processing of V₂AlC MAX phase: Optimization of sintering temperature and composition

Ayomide Adeola Sijuade ^{a,c}, Franchesca Lydia Bellevu ^{a,b}, Sanjay Kumar Devendhar Singh ^b, Md Mostafizur Rahman ^c, Natalie Arnett ^b, Okenwa I. Okoli ^{a,b,c,*}

- ^a High-Performance Materials Institute, Tallahassee, FL, 32310, USA
- ^b FAMU-FSU College of Engineering, Tallahassee, FL, 32310, USA
- ^c Herff College of Engineering, University of Memphis, Memphis, TN, 38111, USA

ARTICLE INFO

Handling Editor: Dr P. Vincenzini

 $\label{eq:continuous_continuous_continuous} Keywords: \\ 2D materials \\ V_2AlC MAX phase synthesis \\ Sintering$

ABSTRACT

The Vanadium MAX phase (V_2AlC) was synthesized by the pressureless sintering method using elemental V, Al, and C powders as starting materials. The synthesis process involves varying the aluminum molar ratios and temperature to fully realize the optimal conditions for MAX phase synthesis. Systematic variation of the aluminum molar ratio in the range of 1.2 to 1.4 reveals that an aluminum ratio of 1.2 minimizes side reactions and compensates for aluminum loss due to the compound's volatility, optimizing Vanadium MAX phase synthesis. Furthermore, this research examines the profound impact of synthesis temperature on the composition and structure of the Vanadium MAX phases. The results indicate that the ideal temperature for achieving maximum yield, phase purity, crystallinity, and the desired microstructure is 1300 °C. Scanning electron microscopy (SEM) analysis reveals the intricate nanolaminate structure of MAX phases, characterized by fluctuations in layer thickness. Notably, we observe an average particle size of 8.27 μ m, with sample 1 and sample 3 exhibiting the largest and smallest sizes at 9.51 μ m and 7.28 μ m, respectively. The highest conductivity, reaching 7.19E-5 S/m, and the purest samples are consistently obtained at 1300 °C with an aluminum ratio of 1.2, reaffirming the optimized conditions. In summary, this research unveils the intricate chemistry of factors influencing the synthesis of Vanadium MAX phases, shedding light on their immense potential and offering new perspectives and possibilities in MAX phase synthesis.

1. Introduction

The discovery of MAX phases, also known as "H- or Hagg phases," due to its hexagonal structure, created a new system, which combined metallic and ceramic properties, that served as the basis for future ternary carbides and nitrides [1,2]. The name MAX comes from the chemical formulation of $M_{n+1}AX_n$ in which M—early transition metals, A—an A-group element (usually between subsets 13-16), and X— which can be either carbon or nitrogen, with the 'n' subscript being a number between 1 and 3 [3]. The phases exhibit the P63/mmc (no.194) space group and are categorized into six groups based on the 'n' value, which can range from a 211 phase to a 716 phase [4,5]. These phases also consist of pure 'A' atoms sandwiched between alternating layers of nearly tightly packed M_6X octahedra. The M_6X octahedra are joined to one another by shared edges and resemble those that arise in the corresponding (MX) binary carbides [6]. MAX phases exhibit stacked

atomic layers with significant metallic and ceramic properties [7]. The attractiveness of these materials is attributed to the properties acquired upon synthesis. Due to the covalent bonding between the layers, MAX phases demonstrate enhanced stiffness, moduli, and high thermal and electrical conductivity, acting like metal conductors with resistance between 0.07 and 2 $\mu\Omega$ m at room temperature [8]. In addition, low thermal expansion coefficients and increased resistance to wear, heat, damage, and thermal shock are also achieved [7,9]. These characteristics differentiate MAX phases from binary carbides and nitrides (MX)

Furthermore, the stiff but soft contrast of the MAX plasticity controls its ability to withstand high levels of compression and tension [10]. These characteristics of MAX phases allow for use in high-temperature applications, protective coatings, sensors, electrical contacts, cladding materials, heat exchangers, sensors, and concentrated solar power applications [11]. Notably, the primary use of MAX phases is as a precursor

^{*} Corresponding author. Herff College of Engineering, University of Memphis, Memphis, TN, 38111, USA. *E-mail address*: O.Okoli@memphis.edu (O.I. Okoli).

in synthesizing MXenes with the general formula $M_{n+1}X_nT_x$ (where T_x denotes surface termination such as O, F, OH). MXenes are synthesized by etching the aluminum layer from the MAX phases [12]. The selective etching process aims to break down the chemical bonds between the M and A elements in the MAX phases, which eventually etches the A elements [12,13]. The synthesized MXenes are ultimately used to fabricate energy storage devices: capacitors, Li-ion batteries, and sensors [14,15].

V₂AlC is the most studied subgroup of the MAX phase in the V-Al-C system compared to other reported subgroups like 312 and 413 [16]. Ghasali et al. studied the spark plasma sintering of V₂AlC and V₄AlC₃ at 1300 °C without aggressive milling conditions [17]. The synthesis procedure produced dense samples, good bending strength, and hardness. However, it was noticed that V₄AlC₃ had slightly higher Vicker's hardness due to higher amounts of Al₂O₃ present [17]. Using a 6.5 M HCl solution, potentiodynamic polarization, and electrochemical impedance spectroscopy (EIS) test, it was found that V₄AlC₃ had a lower corrosion current density than V2AlC [17]. This indicates that V2AlC is less resistant to corrosion compared to V₄AlC₃. In other words, preferential dissolution at grain boundaries or etching of "A" group elements in V₂AlC is higher than in V₄AlC₃, which helps the former form layered MXene structures easily. The self-propagating high-temperature synthesis (SHS) was also used for synthesis due to its short sintering time; Gorshkov et al. revealed that only a 65% yield of V2AlC was obtained [18]. Due to the extremely short reaction time, various intermediate products are formed, like V2C, VAl, VAl3, and VCx. V2AlC prepared through SHS showed good conductive capacity due to forming chains of V₂AlC nanolaminate grains that created a continuous framework in the bulk material [18,19]. Research from Hu et al. showed the synthesis of dense V₂AlC samples with an average density of 4.01 g/cm³. It was reported that the increase in sintering temperature led to larger V₂AlC grains. At 1400 °C, the grain length was 49 μm and width of 19 μm with the highest compressive strength, while at 1700 °C, the length was 405 μm and width of 106 μm with the highest damage tolerance evaluated based on the damage tolerance parameter, D_t (m^{1/2}).

On the other hand, V_2AlC synthesized at 1500 °C exhibited the highest flexural strength (289 MPa) [19]. These results show that the mechanical properties and grain sizes of synthesized V2AlC are temperature-dependent. Based on the available literature, it is essential to highlight that an excess of aluminum is commonly used beyond its stoichiometric requirement to minimize aluminum loss caused by its high vapor pressure at elevated temperatures [19]. However, the optimized aluminum ratio needed for synthesizing the V₂AlC MAX phase was still unconfirmed, which is crucial for forming an effective V₂AlC MAX phase. Hence, this study focuses on optimizing the Al element in the composition of the V2AlC MAX phase. Due to the numerous advantages like its simplicity, high purity, and high heating rate, the pressure-less sintering method was utilized to synthesize V₂AlC in this study. An experiment was designed to optimize the sintering temperature and aluminum ratio to minimize the side reactions that would decrease the electrical conductivity of the MAX phases.

2. Experimental procedure

2.1. Materials

MAX phases were synthesized with vanadium powder (V, 99.5%, -325 mesh), aluminum powder (Al, 99.5%, 60 μm), and graphite powder (C, 99%, -325 mesh) purchased from Millipore Sigma. The design of the experiments is presented in Table 1. It consists of 6 trials with varying sintering temperatures and aluminum stoichiometric ratios with constant vanadium and carbon content. The design considered two aluminum molar ratios (V: Al: C = 2:1.2:1, and 2:1.4:1) and three sintering temperatures, 1150, 1300, and 1450 °C. Each sample with temperatures and aluminum ratios is assigned a sample number in column 1 of Table 1.

Table 1 Experimental design for MAX phase synthesis.

Sample No.	Molar r	atio	Temperature (°C)	
	V	Al	С	
1	2	1.2	1	1150
2	2	1.2	1	1300
3	2	1.2	1	1450
4	2	1.4	1	1150
5	2	1.4	1	1300
6	2	1.4	1	1450

2.2. Methods

Six batches of the V₂AlC MAX phase were prepared with varying compositions and temperatures using the pressureless sintering method. Each sample with its respective elemental composition was ball milled in a stainless-steel grinding vial set with four ½ inch stainless steel balls for 4 h. The powders were pressed into 0.56 g pellets via a hydraulic press at 400 kPa for 1 min. The powder batch yielded 5-6 pellets sintered inside two ceramic crucibles. The green pellets were sintered in an alumina tube furnace with a heating rate of 300 $^{\circ}$ C/min to the respective furnace temperatures, with a holding time of 5 h in flowing argon gas. The sintered monoliths were crushed with a mortar and pestle to produce MAX phase powder.

2.3. Characterization

2.3.1. XRD

The phases of samples were studied using the X-ray powder diffraction (XRD) test using a Rigaku RAD diffractometer in Bragg-Brentano geometry using Cu K α radiation with accelerating voltage and applied emission currents of 40 kV and 30 mA, respectively. The scanning angle (20) was set from 10° to 80° . The acquired data were analyzed using the Rietveld method to determine the present phases and lattice parameters. This refinement was done using the GSAS II software. The refined parameters, such as lattice parameters of all the phases, background parameters, and scale factors, were used to evaluate the relative phase fractions.

2.3.2. SEM

The microstructure of the particles was confirmed by a scanning electron microscope (SEM Phenom XL Desktop SEM) with an accelerating voltage of 15.0 kV in the secondary electron (SE) imaging mode. The SEM was set with an energy-dispersive X-ray spectrometry (EDS) to understand the elemental composition. This was done without any Au coating as the samples are conductive.

2.3.3. Raman spectroscopy

Raman spectroscopy was carried out by a confocal microscope (Renishaw in Via reflex confocal Raman microscope) with a 633 nm wavelength and a power of 0.5 mW. The laser beam focus had a 50X magnification objective lens with a laser beam size of about 10 μ m.

2.3.4. TEM

The scanning transmission electron microscope (STEM) imaging was carried out using the probe Cs corrected cold field-emission gun JEOL JEM-ARM200F equipped with an EDAX detector, an Orius camera, an Ultrascan camera, and STEM detectors. STEM imaging and elemental analysis were performed in a probe-corrected atomic resolution analytical electron microscope (JEM-ARM200cF, JEOL) with an energy dispersive X-ray spectroscopy (EDS) detector (X-MaxN 100TLE SDD, Oxford Instruments). The STEM images were taken with a probe size of 0.078 nm, a probe current of 23 pA, and a collection angle of 90–174.6 mrad, as the differential pumping aperture between the column and the camera chamber limits the outside collection radius.

2.3.5. Electrical conductivity

The electrical conductivity measurements were done using pelletized powder samples weighing 0.5g with a Jandel universal four-point probe station. A Keithley 6221 current source and a 2182 nanovoltmeter with current-voltage characteristics were used. The measurements were done by inserting four probes into the pellet sample, where current passes through the outer probes and voltage is induced through the inner probes. The measuring process was repeated 10 times, and an average of this measurement is reported here.

3. Results and discussion

The temperatures utilized for synthesis were 1150,1300, and 1450 $^{\circ}$ C with aluminum molar ratios of 1.2 and 1.4. The formation of MAX phases starts around 1000 $^{\circ}$ C, and the highest yield is achieved between 1300 $^{\circ}$ C and 1400 $^{\circ}$ C [1]. Hence, the different temperatures and ratios were used to find the optimum conditions for achieving the highest yield is used in this study. The run order would denote the samples as seen in the design of experiment in Table 1.

3.1. Reaction synthesis and phase evolution

$$G_{VAIC}^{V2AIC} = 2G_V^{bcc} + G_{AI}^{fcc} + G_C^{graphite} - 198,000$$
 (1)

$$G_{V:AlC:C}^{V:AlC:C} = 4G_V^{bcc} + G_{Al}^{fcc} + 3G_C^{graphite} - 378,000$$
 (2)

The MAX phase has an H-phase crystal structure in which two layers of vanadium and one layer of aluminum alternately form hexagonal packings. The C layers fill the octahedral voids between the V layers [20]. One unit cell of V_2AlC contains eight atoms, with V atoms positioned at (1/3, 2/3, u), Al atoms at (1/3, 2/3, 3/4), and the C atoms at (0,0,0), where u is an optimized internal coordinate parameter of the V atom [21]. The thermodynamic parameters for the formation of V_2AlC and V_4AlC_3 are shown in equations (1) and (2) below [22].

Thermodynamic calculations show that the Gibbs free energy of the reaction for equation (3) is all negative at temperatures ranging from 273 to 1673K, which shows that the reaction using elemental powders occurs spontaneously [23]. This also suggests that it is easier to synthesize V_2AIC with reduced aluminum content using elemental powders in comparison to the synthesis using equation (4).

$$2V + AI + C = V_2AIC \tag{3}$$

$$Al_4C_3 + 6Al_3V = V_2AlC + 19Al$$
 (4)

Hu et al. proposed equations (5)–(7) as the reactions that lead to the formation of V₂AlC, corresponding to the results obtained [19]. Al is believed to first react with V to form Al₃V at 700 °C. As the temperature rises, Al₃V and V react to form Al₈V₅ (eqn. (6)). Between 1000 and 1200 °C, V₂AlC starts to emerge alongside VC (eqn. (7)). Around 1300 °C, the concentration of VC and V₂AlC starts to increase while the amount of Al₈V₅ and C decreased [19]. With further rise in temperature to 1400 °C, the dominant phase was found to be V₂AlC along with some impurities such as VC and V₄AlC₃ impurities (eqn. (7)). The plausible mechanism for V₄AlC₃ could be due to the reaction of V₂AlC with VC. To

ascertain the above claim, in this study, Rietveld analysis of all samples was carried out to compute the phase fraction.

$$V + 3AI = AI_3V \tag{5}$$

$$8Al_3V + 7V = 3Al_8V_5 (6)$$

$$Al_8V_5 + 3C = 2V_2AlC + VC + 6Al$$
 (7)

Table 2 shows the volume fraction of the synthesized MAX phases obtained from the Rietveld refinement using the GSAS II software. It also confirms that sample 1 had the lowest yield, demonstrating that an increase in temperature increases the yield of the MAX phase. The results also confirm that sample 1 had the lowest yield, indicating that an increase in temperature increases the yield of the MAX phase. This agrees with Wang et al. [24], which shows that an increase in the temperature from 1050 $^{\circ}\text{C}$ to 1400 $^{\circ}\text{C}$ increased the phase purity and yield. Additionally, it is worth noting that the self-propagation high-temperature synthesis (SHS), hot pressing, and spark plasma sintering (SPS) methods all necessitate temperatures exceeding 1200 $^{\circ}\text{C}$ for the most effective synthesis to take place [1].

Observations from this study show that the MAX phase had the highest yield in sample 2; the experiment was performed at $1300\,^{\circ}\text{C}$ and had an aluminum ratio of 1.2. Table 2 also confirms the presence of $V_4\text{AlC}_3$ in all except sample 6. This reaction increases the vanadium carbide (VC) content, which reacts with the already synthesized $V_2\text{AlC}$ to form $V_4\text{AlC}_3$ through diffusion and interface migration. This reaction is likely due to increased Frank partial dislocation behavior [25]. Despite high-purity argon flow during sintering, oxides of vanadium and aluminum may develop due to surface-adsorbed oxygen/CO₂, which might have reacted with the metallic powders during sintering [16].

Fig. 1 shows the XRD patterns of the synthesized MAX phases with varying molar ratios at the respective furnace temperatures of 1150, 1300, and 1450 $^{\circ}$ C. As illustrated, the peaks of the V₂AlC are visible at $13.4^{\circ},\,35.5^{\circ},\,36.2^{\circ},\,41.3^{\circ},\,55.5^{\circ},\,63.8^{\circ},\,75.1^{\circ},\,78.9^{\circ}$ which corresponds to (002), (100), (101), (103), (106), (110), (109), and (203) planes respectively. This demonstrates the successful synthesis of the V₂AlC MAX phase. The intensity of the peaks is low when the experiment was conducted at low temperatures,1150 °C, which indicates that synthesis of V₂AlC MAX phases at 1150 °C could result in a high quantity of impure phases. Increasing the Al concentration did not bring any substantial changes in V₂AlC formation. It was observed that more impurities were formed when the Al concentration was increased to 1.4 at the same temperature (1150 °C). On the other hand, the 1.2 aluminum molar ratio sample sintered at 1300 °C (sample 2) exhibited the most visible peaks of the V2AlC with the least amount of different visible elemental combinations. Table 3 shows the lattice parameters of the synthesized V2AlC samples from this study with that of literaturereported values. The Rietveld refined diffractograms of all the samples and derived parameters, such as weighted profile R values (Rwp) and goodness of fit (GoF), are presented in the supplementary material (Figs. S1–S6 and Table T1). Table 3 confirms that the lattice parameters derived from this study were comparable to those of literature-reported values.

Fig. 2 illustrates the Raman spectra of the synthesized samples. This was carried out as supporting information for the V_2AIC phase

Table 2 Volume fraction of different phases in the prepared V_2AlC MAX phases.

MAX phase sample	Sintering Temperature $^{\circ}\text{C}$	Percentage							
		V ₂ AlC	Al_2O_3	V ₄ AlC ₃	V ₈ C ₇	V ₃ O ₅	V_2O_3	V_2	V ₂ C
1	1150	73.73	6.17	0.87	1.91	13.11	4.22	-	-
2	1300	94.38	5.15	0.16	-	0.32	-	-	-
3	1450	92.07	6.66	1.09	0.13	-	-	0.05	-
4	1150	83.24	11.87	0.84	0.23	-	-	0.23	3.58
5	1300	90.99	7.64	0.18	-	-	0.16	1.03	-
6	1450	93.81	5.85	-	0.09	0.26	-	-	-

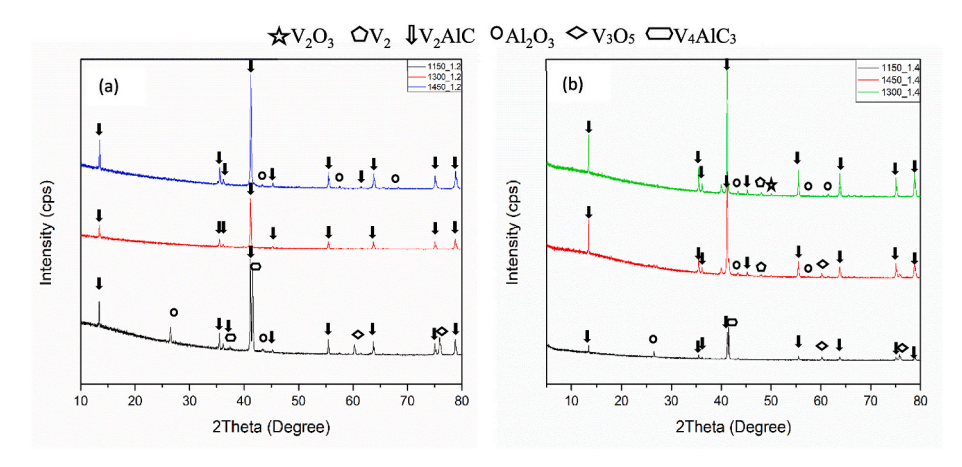


Fig. 1. XRD patterns of V_2AlC samples prepared using Al molar ratio of (a) 1.2 and (b) 1.4.

 $\label{eq:control_control_control} \textbf{Table 3} \\ \textbf{Lattice parameters of synthesized V_2AlC samples.}$

	_	
a (Å)	c (Å)	Reference
2.9192	13.158	This work
2.9181	13.158	
2.9147	13.144	
2.9183	13.150	
2.9176	13.149	
2.9186	13.156	
2.9000	13.14	[8]
2.9120	13.157	[26]
2.9107	13.101	[20]
2.9090	13.120	[27]
2.9120	13.140	[28]
	2.9192 2.9181 2.9147 2.9183 2.9176 2.9186 2.9000 2.9120 2.9107 2.9090	2.9192 13.158 2.9181 13.158 2.9147 13.144 2.9183 13.150 2.9176 13.149 2.9186 13.156 2.9000 13.14 2.9120 13.157 2.9107 13.101 2.9090 13.120

formation. The characteristic (V-V) and (V-Al) peaks of V_2AlC can be seen in all samples at different intensities. In Fig. 2a and b, the carbide compounds are responsible for bands close to 138 and 630 cm⁻¹. The vibrational motion of V-O bonds is observed at 281 cm⁻¹. Al-O and vanadyl (V=O) stretching bonds can be seen at 400 and 1000 cm⁻¹ bands, respectively [8]. Fig. 2c shows the highest percentage of V_2AlC , with the Al-V and V-V vibrational modes having the highest intensity compared to other samples, confirming that it is the most optimized condition for synthesizing V_2AlC as seen in work by Mothare et al. [8].

3.1.1. Microstructure analysis

The morphology of MAX powders derived from different temperatures and aluminum ratios is presented in Fig. 3. The SEM images display the formation of a nanolaminate structure with the typical layered stacked structure of the MAX phases in all the samples. However, the nanolaminate layers' thickness is non-uniform, as observed in Fig. 3e. Fig. 3a and d, synthesized at $1150\,^{\circ}\text{C}$, show that the layered structure is

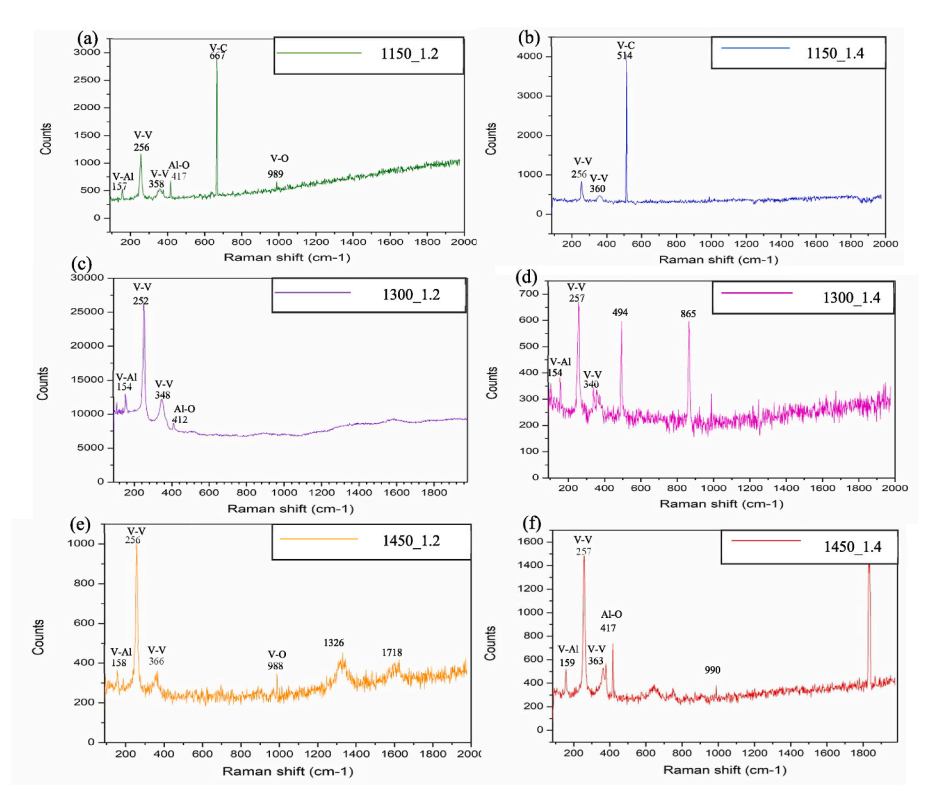


Fig. 2. Raman spectra of samples synthesized with the 1.2 aluminum ratio.

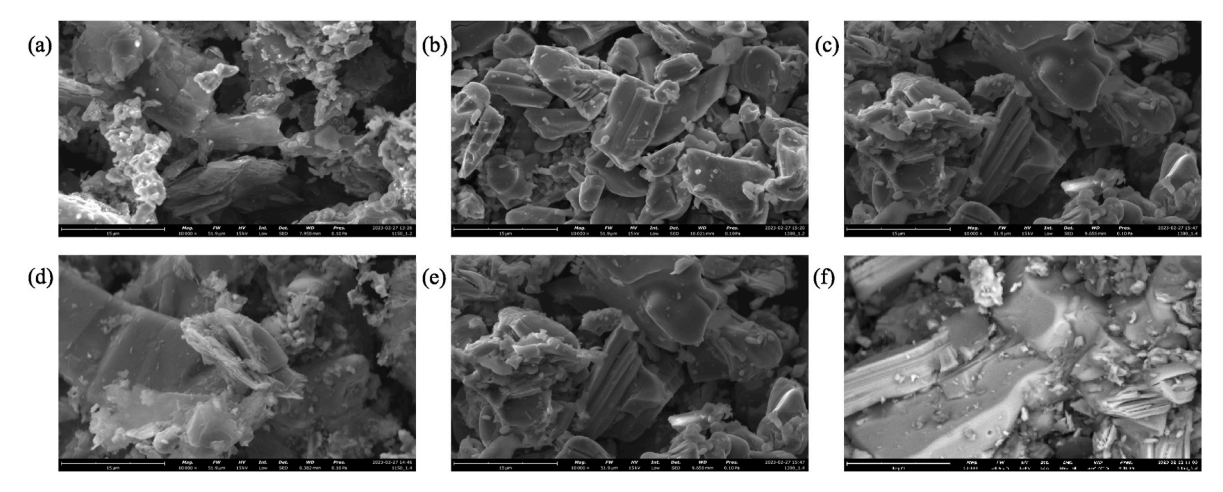


Fig. 3. SEM micrographs of MAX phase: (a)sample 1 (b) sample 2 (c) sample 3 (d) sample 4 (e) sample 5 (f) sample 6.

not as pronounced as samples 2, 3, 5, and 6 synthesized at 1300 $^{\circ}C$ and 1450 $^{\circ}C$ which could be due to incomplete reaction of the MAX phase. The average particle size of the MAX phases was measured at 8.27 μm . Within this set of samples, sample 1 had the largest size at 9.51 μm , while sample 3 displayed the smallest particle size at 7.28 μm .

TEM images shown in Fig. 4 confirm the moire pattern and stacked structure of V_2 AlC. It also ensures the strong intergrowth of the particles often depicted with the hexagonal shape [29]. From Fig. 4c, the layered structure of the MAX phases is predominant, which signifies the optimized temperature and molar ratio at 1300 °C and 1.2, respectively.

3.2. Conductivity test

The conductivity tests were performed 10 times, and the average was reported. It is well known that electrical conductivity depends on the particle packing, mean crystallite, particle size distribution, and the chemical nature of individual particles in the powders [8]. From Fig. 5,

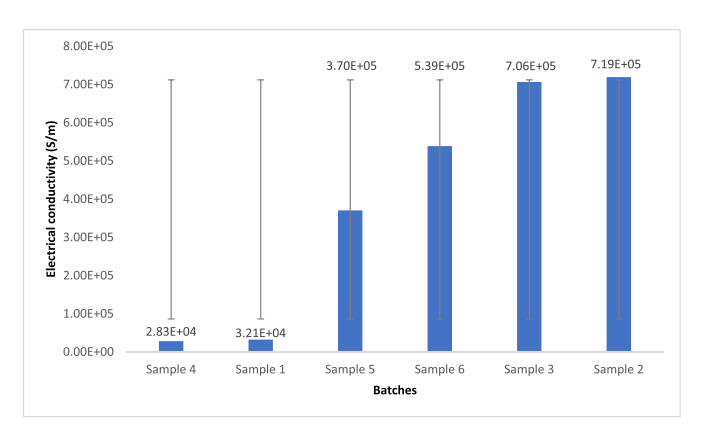


Fig. 5. Conductivity graph of synthesized MAX phases.

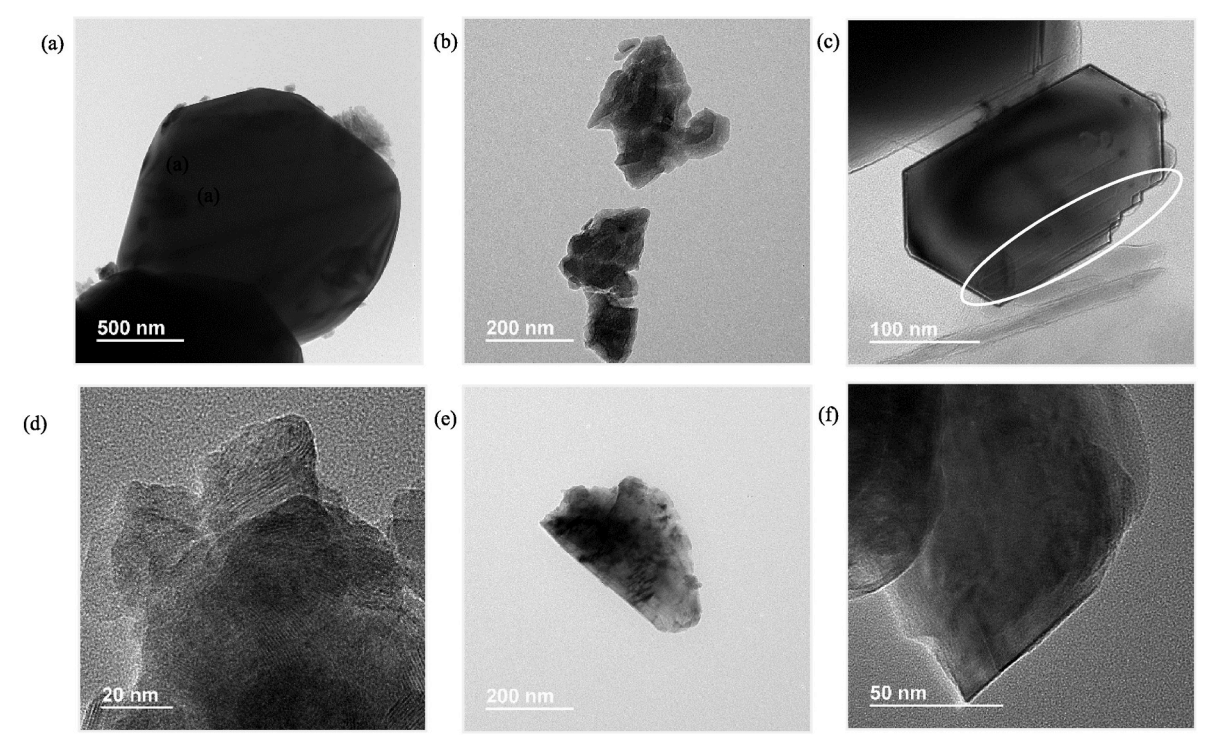


Fig. 4. TEM micrographs of MAX phase: (a)sample 1 (b) sample 2 (c) sample 3 (d) sample 4 (e) sample 5 (f) sample 6.

the highest and lowest conductivities are attributed to samples 2 and 4 with temperature and aluminum ratios of $1300\,^{\circ}\text{C}$, 1.2 and $1150\,^{\circ}\text{C}$, 1.4, respectively. Given that the samples had the lowest and highest amounts of Al_2O_3 , respectively, the high and low conductivities may be attributed to the non-conductive properties of Al_2O_3 . In addition, the conductivity of the MAX phases increases with an increase in the density, as seen in work by Motahare et al. [8]. Samples 2 and 4 had a 2.26 and $1.48\,\text{kg/m}^2$ density, respectively. Also, the MAX phases synthesized at $1150\,^{\circ}\text{C}$ had the lowest conductivity, which can be linked to the incomplete synthesis of the MAX phases. In addition, the MAX phase synthesis. Therefore, from the discussion, it may be postulated that increasing the sintering temperature improves the electrical conductivity of the vanadium MAX phases.

4. Conclusion

In conclusion, the synthesis at various temperatures and compositions (molar ratios) has gained significant knowledge of MAX phases' structural and functional characteristics. Based on a series of experiments derived from the experiment design, the best aluminum ratio for obtaining the requisite MAX phase qualities is 1.2, with a synthesis temperature of 1300 °C. It was discovered during the investigation that the aluminum ratio significantly affects the final properties of the MAX phases. The higher the aluminum ratio, the more side reactions were observed in the synthesized samples. The synthesis temperature significantly influenced the final composition and structure of the MAX phases. A well-balanced combination of MAX phase qualities, including phase purity, crystallinity, and desirable microstructure, was discovered to be best at a temperature of 1300 °C.

Additional study and testing are required to understand the underlying mechanisms and potential differences in MAX phase properties concerning various aluminum ratios and synthesis temperatures. By increasing our knowledge and employing MAX phases more effectively, further research in this field will help them realize their full potential across various technical sectors.

Declaration of competing interest

The authors declare that they have no known competing financial interests or personal relationships that could have appeared to influence the work reported in this paper.

Acknowledgments

This work was supported by research funds from the NSF Excellence in Research Award (Grant number DMR-2101001) and the DoE Minority Serving Institution Partnership Program (Grant number DE-NA0004004).

Appendix A. Supplementary data

Supplementary data to this article can be found online at https://doi.org/10.1016/j.ceramint.2023.11.126.

References

- J. Gonzalez-Julian, Processing of MAX phases: from synthesis to applications,
 J. Am. Ceram. Soc. 104 (2) (2021) 659–690, https://doi.org/10.1111/jace.1754
- [2] M.W. Barsoum, The Mn+1 AXn phases and their properties, in: R. Riedel, I.-W. Chen (Eds.), Ceramics Science and Technology, Wiley-VCH Verlag GmbH & Co. KGaA, Weinheim, Germany, 2010, pp. 299–347, https://doi.org/10.1002/9783527631735.ch7.
- [3] T. Lapauw, et al., Synthesis of the new MAX phase Zr2AlC, J. Eur. Ceram. Soc. 36 (8) (Jul. 2016) 1847–1853, https://doi.org/10.1016/j.jeurceramsoc.2016.02.044.

- [4] M.W. Barsoum, M. Radovic, Elastic and mechanical properties of the MAX phases, Annu. Rev. Mater. Res. 41 (1) (Aug. 2011) 195–227, https://doi.org/10.1146/ annurey.mateci.062010.100448
- [5] X.K. Qian, Methods of MAX-phase synthesis and densification I, in: Advances in Science and Technology of Mn+1AXn Phases, Elsevier, 2012, pp. 1–19, https://doi. org/10.1533/9780857096012.1.
- [6] Z. Sun, H. Hashimoto, W. Tian, Y. Zou, Synthesis of the MAX phases by pulse discharge sintering, Int. J. Appl. Ceram. Technol. 7 (6) (2010) 704–718, https:// doi.org/10.1111/j.1744-7402.2010.02555.x.
- [7] Synthesis and Physical Properties of (Zr1-x,Tix)3AlC2 MAX Phases Zapata-Solvas, Journal of the American Ceramic Society Wiley Online Library, 2017. Accessed: Mar. 01, 2023. [Online]. Available: https://ceramics.onlinelibrary.wiley.com/doi/10.1111/jace.14870.
- [8] M.S. Mohseni-Salehi, E. Taheri-Nassaj, A. Babaei, M. Soleimanzade, Effect of different precursors on the formation and physical properties of V2AIC MAX phase, J. Alloys Compd. 918 (Oct. 2022), 165588, https://doi.org/10.1016/j. iallcom.2022.165588.
- [9] C. Roy, P. Banerjee, S. Bhattacharyya, Molten salt shielded synthesis (MS3) of Ti2AlN and V2AlC MAX phase powders in open air, J. Eur. Ceram. Soc. (2019), https://doi.org/10.1016/j.jeurceramsoc.2019.10.020.
- [10] M. Radovic and M. W. Barsoum, "MAX phases: bridging the gap between metals and ceramics," MAX Phases, vol. 92, no. 3, p. 8.
- [11] P. Sharma, K. Singh, O.P. Pandey, Investigation on oxidation stability of V2AlC MAX phase, Thermochim. Acta 704 (2021), 179010, https://doi.org/10.1016/j. tca.2021.179010. Oct.
- [12] A.A. Sijuade, V.O. Eze, N.Y. Arnett, O.I. Okoli, Vanadium MXenes materials for next-generation energy storage devices, Nanotechnology 34 (25) (2023), 252001, https://doi.org/10.1088/1361-6528/acc539. Apr.
- [13] C. Zhou, et al., A review of etching methods of MXene and applications of MXene conductive hydrogels, Eur. Polym. J. 167 (Mar. 2022), 111063, https://doi.org/ 10.1016/j.eurpolymj.2022.111063.
- [14] L. Fu, W. Xia, MAX phases as nanolaminate materials: chemical composition, microstructure, synthesis, properties, and applications, Adv. Eng. Mater. 23 (4) (2021), 2001191, https://doi.org/10.1002/adem.202001191.
- [15] S. Gao, N. Miao, J. Zhou, Synthesis and Characterization of High Purity V2AlC Prepared by Pressureless Sintering, 44, Beijing Hangkong Hangtian Daxue XuebaoJournal Beijing Univ. Aeronaut. Astronaut., Apr. 2018, pp. 868–873, https://doi.org/10.13700/j.bh.1001-5965.2017.0295.
- [16] M. Hossein-Zadeh, O. Mirzaee, H. Mohammadian-Semnani, An investigation into the microstructure and mechanical properties of V4AlC3 MAX phase prepared by spark plasma sintering, Ceram. Int. 45 (6) (Apr. 2019) 7446, https://doi.org/ 10.1016/j.ceramint.2019.01.036. –7457.
- [17] E. Ghasali, M.R. Derakhshandeh, Y. Orooji, M. Alizadeh, T. Ebadzadeh, Effects of 211 and 413 ordering on the corrosion behavior of V-Al-C MAX phases prepared by spark plasma sintering, J. Eur. Ceram. Soc. 41 (9) (Aug. 2021) 4774–4787, https:// doi.org/10.1016/j.jeurceramsoc.2021.03.001.
- [18] V.A. Gorshkov, A.V. Karpov, D. Yu Kovalev, A.E. Sychev, Synthesis, structure and properties of material based on V2AlC MAX phase, Phys. Met. Metallogr. 121 (8) (Aug. 2020) 765–771, https://doi.org/10.1134/S0031918X20080037.
- [19] C. Hu, et al., In situ reaction synthesis and mechanical properties of V2AlC, J. Am. Ceram. Soc. 91 (12) (2008) 4029–4035, https://doi.org/10.1111/j.1551-2916.2008.02774.x.
- [20] J. Etzkorn, M. Ade, H. Hillebrecht, V2AlC, V4AlC3-x (x \approx 0.31), and V12Al3C8: synthesis, crystal growth, structure, and superstructure, Inorg. Chem. 46 (18) (Sep. 2007) 7646–7653, https://doi.org/10.1021/ic700382y.
- [21] Z. Yang, et al., Lattice instability of V2AlC at high pressure, Sci. China Phys. Mech. Astron. 56 (5) (May 2013) 916–924, https://doi.org/10.1007/s11433-013-5055-z.
- [22] B. Hallstedt, Thermodynamic evaluation of the Al-V-C system, Calphad 41 (Jun. 2013) 156–159. https://doi.org/10.1016/j.calphad.2013.03.002.
- 2013) 156–159, https://doi.org/10.1016/j.calphad.2013.03.002.
 [23] L. Wei, X. Liu, Y. Gao, N. Hu, "Thermodynamic analysis and synthesis of V2AlC phase material," in *TMS 2022 151st annual meeting & exhibition supplemental proceedings*, in: The Minerals, Metals & Materials Series, Springer International Publishing, Cham, 2022, pp. 1497–1504, https://doi.org/10.1007/978-3-030-92381-5-142
- [24] B. Wang, A. Zhou, Q. Hu, L. Wang, Synthesis and oxidation resistance of V2AlC powders by molten salt method, Int. J. Appl. Ceram. Technol. 14 (5) (2017) 873–879, https://doi.org/10.1111/ijac.12723.
- [25] Y. Zhong, Y. Liu, J. Ye, N. Jin, Z. Lin, Molten salt synthesis and formation mechanisms of ternary V-based MAX phases by V-Al alloy strategy, J. Am. Ceram. Soc. 105 (3) (2022) 2277–2287, https://doi.org/10.1111/jace.18198.
- [26] A. Abdulkadhim, et al., Crystallization kinetics of V2AIC, Thin Solid Films 520 (6) (Jan. 2012) 1930–1933, https://doi.org/10.1016/j.tsf.2011.09.037.
- [27] J.C. Schuster, H. Nowotny, C. Vaccaro, The ternary systems: CrAlC, VAlC, and TiAlC and the behavior of H-phases (M2AlC), J. Solid State Chem. 32 (2) (Apr. 1980) 213–219, https://doi.org/10.1016/0022-4596(80)90569-1.
- [28] H.O. Badr, A. Champagne, T. Ouisse, J.-C. Charlier, M.W. Barsoum, Elastic properties and hardness values of V 2 AlC and C r 2 AlC single crystals, Phys. Rev. Mater. 4 (8) (Aug. 2020), 083605, https://doi.org/10.1103/ PhysRevMaterials.4.083605.
- [29] E.P. Simonenko, et al., Synthesis of MAX phases in the Ti2AlC–V2AlC system as precursors of heterometallic MXenes Ti2 – xVxC, Russ. J. Inorg. Chem. 67 (5) (May 2022) 705–714, https://doi.org/10.1134/S0036023622050187.